

## Optimum Applications of Four-Port Wave Rotors for Gas Turbines Enhancement

### Emmett Dempsey

Michigan State University  
Dept. of Mechanical Engineering  
2500 Engineering Building  
East Lansing, Michigan 48824-1226  
Phone: (517) 432 9139  
Fax: (347) 412 7848  
Email: dempse11@msu.edu

### Pezhman Akbari

Purdue School of Eng. and Technology  
Dept. of Mechanical Engineering  
723 West Michigan Street  
Indianapolis, Indiana 46202-5132  
Phone: (317) 278 3010  
Fax: (317) 274 9744  
Email: akbari@iupui.edu

### Norbert Müller

Michigan State University  
Dept. of Mechanical Engineering  
2455 Engineering Building  
East Lansing, Michigan 48824-1226  
Phone: (517) 432 9139  
Fax: (347) 412 7848  
Email: mueller@egr.msu.edu

### Razi Nalim

Purdue School of Eng. and Technology  
Dept. of Mechanical Engineering  
723 West Michigan Street  
Indianapolis, Indiana 46202-5132  
Phone: (317) 278 3010  
Fax: (317) 274 9744  
Email: mnalim@iupui.edu

### Abstract

Many investigations on wave rotor applications for gas turbines have been published, among them conceptual, analytical, numerical and supporting experimental work. They have reported the benefits of wave rotor implementations supported by promising tests, but rarely with general trends. Frequently, it has been asked where the most appropriate design space is in which the wave rotor application is most beneficial.

This investigation aims to answer this question comprehensively and be readily applicable for initial development decisions in the gas turbine industry. The results and conclusions are derived from a wide-range multi-parameter investigation based on a cycle thermodynamic analysis coupled with the wave rotor characteristic equation [1]. Multi-parametric performance maps for different wave rotor implementations have been generated specifying optimum operating points for both untopped baseline engine and topped engine employing the most conventional form of the wave rotor: the four-port wave rotor. Important design parameters like turbine inlet temperature, cycle pressure ratio, component efficiencies and losses are varied in a systematic performance analysis. The presented results allow identifying the optimum design point of wave-rotor-enhanced gas turbines from which best operating ranges can be determined initially, depending on the expected component performances. Obtained results can be useful in demonstrating the potential of wave

rotors, encouraging further developments in this promising technology. General design guidelines contribute to the practical value of this work.

### Nomenclature

#### Symbols and Abbreviations

OPR	overall pressure ratio
PRW	wave rotor compression ratio
R	compressor pressure ratio
SFC	specific fuel consumption
w	specific work
T	temperature
$\eta$	efficiency
$\Pi$	pressure ratio

#### Subscripts

b	baseline (untopped) engine
comb	combustor loss
PC	polytropic compressor
PT	polytropic turbine
th	thermal
WE	wave rotor expansion
WP	wave rotor compression
3	combustor outlet
4	turbine inlet

## Introduction

Especially for aerospace applications, recently there has been considerable interest in enhancing or even substituting turbomachinery with unsteady-flow machines that utilize compression and expansion waves. While there are extensive efforts in developing multi-tube or rotary pulse detonation engines (PDE) to enhance and exceed the performance of gas turbines, the wave rotor technology is still a favorable alternative allowing performance improvement beyond the limits set by restricted turbine inlet temperatures and other relevant design considerations. Despite considerable research yielding highly favorable results, commercialization of the wave rotor for gas turbine applications has not yet been achieved, mostly due to circumstances other than the remaining technical challenges.

A wave rotor is an unsteady flow device that uses shock waves to pressurize a fluid. It consists of curved or straight channels in a rotating drum or disc. A schematic picture of a wave rotor can be seen in Fig. 1. At both ends of the channels are end plates that have ports. The number of ports can vary, but this investigation focuses on four ports per cycle; two of them in each end plate. Each port is designed to open the channels at a specific shaft angle and for a specific duration. Shock waves are initiated inside the channels by sudden pressure differences introduced by the port opening and closing. Since the channels are exposed to both hot and cool gases, wave rotors are self-cooling [2]. This is especially important in gas turbine applications where the turbine inlet temperature is limited by material constraints [3]. Because of the expansion in the wave rotor and its self-cooling qualities, the combustor can operate at higher temperatures without raising the turbine inlet temperature. Thus the efficiency of the entire cycle can be increased.

The usefulness of wave rotors is driven by the fact that advances in gas turbine engine technology have progressed to the point where few or no more significant increases in component efficiencies or material properties can be expected [4]. The addition of a wave rotor allows for significant performance enhancements and possible reduction of material

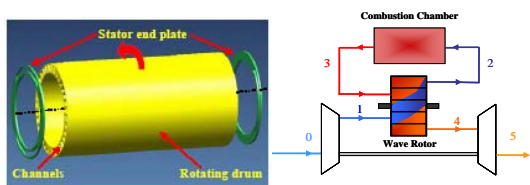


**Figure 1.** Geometry of a wave rotor and its location in a gas turbine engine application .

costs due to changes in pressure and temperature throughout the cycle.

Wave rotors have been studied since the early 1900's, and the benefits are well understood in numerous published works. Yet, wave rotors have not received significant commercialization for gas turbines. However, in the automobile industry internal combustion engines have benefited from wave rotor addition in the form of the Comprex®. 150,000 of Mazda's 626 powered by a diesel engine have been supercharged with a Comprex® pressure wave supercharger [5]. Part of the reason why there has been no significant commercialization of wave rotors as applied to gas turbines may be that not much has been disseminated about the optimum design space for wave rotor application in gas turbines. Therefore, the goal of this study was to create and analyze multi-parametric performance maps for several different cases of wave rotor application in order to determine the optimum design space.

Five different wave rotor-topping cases were investigated in this study. The thermodynamic cycle for each case is shown in Fig. 2. In this figure the numbers represent the cycle stations, while the subscripts represent the cases. Station 0 in the cycle is the compressor inlet, 1 is the compressor outlet/wave rotor inlet, 2 is the wave rotor outlet/combustor inlet, 3 is the combustor outlet/wave rotor inlet, 4 is the wave rotor outlet/turbine inlet, and 5 is the turbine outlet.

- **Case A:** compressor is kept the same as in the baseline (untopped) engine, and turbine inlet temperature ( $T_4$ ) is the same as baseline turbine inlet temperature ( $T_{4b}$ ). The addition of a wave rotor permits combustion at higher temperature up to ( $T_3$ ) for the same amount of heat addition, raising the efficiency and work while lowering the

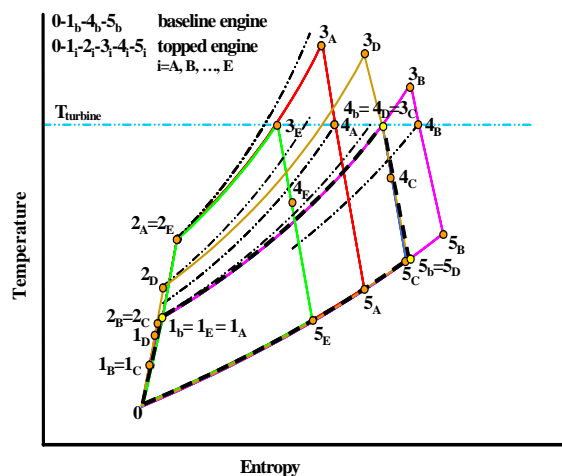


**Figure 2.** Thermodynamic cycle for 5 cases of wave rotor –topped gas turbine engines [4].

fuel consumption of the cycle.

- **Case B:** the overall pressure ratio (OPR) and  $T_4$  are kept same as in the baseline engine. More power is developed while the compressor and turbine each operate at lower pressure ratio, allowing for smaller size and costs. With the highest turbine exit temperature this case is interesting for heat recovery.
- **Case C:** the combustor is unmodified and operates with the same parameter values as in the baseline engine. Performance increases are negligible, but lower pressure ratios in the compressor and turbine, as well as lower turbine inlet temperature allow for smaller size and costs. .
- **Case D:** The turbine operates under exact same temperatures and pressures as in the baseline engine. While this case is similar to case A, the lower pressure ratio in the compressor may allow for some size and cost savings.
- **Case E:** compressor and  $T_3$  are kept the same as in the baseline engine. This case reduces the thermal requirements on the turbine. Similar to cases A, B, and D, there is an increase in work and efficiency plus a decrease in fuel consumption.

## Approach

### Theory

Several steps were involved in the creation of the multi-parametric optimum performance maps. Akbari et al. [6] has presented a procedure for generating general performance maps for fixed turbine inlet temperature or combustor outlet temperature and fixed component efficiencies. This procedure yields three optimum points per wave rotor pressure ratio (PRW). One optimum point has been for thermal efficiency ( $\eta_{th}$ ), one for specific work ( $w$ ), and one for specific fuel consumption (SFC). Hence each of the three optimized objective parameters is a function of the component efficiencies, temperatures, PRW, and compressor pressure ratio  $R$ . For the given procedure, every variable except  $R$  have been fixed. The optimum point on the  $w$  curve is the maximum, which occurs at the  $R$  value where

$$\delta w / \delta R = 0 \quad (1)$$

and

$$\delta^2 w / \delta R^2 < 0 \quad (2)$$

Similarly for  $\eta_{th}$  the optimum occurs at the  $R$  value where

$$\delta \eta_{th} / \delta R = 0 \quad (3)$$

and

$$\delta^2 \eta_{th} / \delta R^2 < 0 \quad (4)$$

Because the optimum SFC is the minimum of the SFC values, it occurs mathematically at the  $R$  value where

$$\delta SFC / \delta R = 0 \quad (5)$$

and

$$\delta^2 SFC / \delta R^2 > 0 \quad (6)$$

By utilizing the partial derivatives represented by equations 1-6, only one particular optimum for the independent variable  $R$  is found. Therefore, the goal in the present work was to create performance maps that display only optimum points of gas turbines with varying combinations of component efficiencies operating under various turbine inlet and combustor outlet conditions.

While each case is different from any of the other cases, they still share some common characteristics with other cases. As observed in Ref. [6], performance data for cases A, B, and D can be displayed in one map sharing one major set of data. Similarly, performance data for cases C and E can be displayed together sharing another major set of data. The main similarity between cases A, B, and D is that they all maintain the same turbine inlet temperature  $T_4$  as the baseline engine  $T_{4b}$ . For cases C and E, the main similarity is that the combustor end temperature  $T_3$  is maintained the same as the turbine inlet temperature of the baseline engine  $T_{4b}$ .

The investigation applies to four-port wave rotors for both through-flow and reverse-flow configuration. In through-flow configuration, gas enters the wave rotor at one end of a channel and exits at the opposite end. In reverse-flow configuration, gas enters and exits the wave rotor at the same end of a channel. Also, because most wave rotor investigations have been performed for pressure ratios of around 1.8, a maximum of 2 was used in this investigation. However that does not necessarily mean that 2 is the maximum achievable wave rotor pressure ratio.

### Method

In order to create a performance map that displays all of the optimum points in the practical domain, layer upon layer of optimum point calculations needed to be created, each layer with a different combination of fixed engine parameters, shown in Table 1. The most practical approach with

<i>Independent Variables</i>	
<b>Cases A, B, and D</b>	<b>Cases C and E</b>
$T_4$	$T_3$
$\eta_{PC}$	$\eta_{PC}$
$\eta_{PT}$	$\eta_{PT}$
$\eta_{WE}$	$\eta_{WE}$
$\eta_{WP}$	$\eta_{WP}$
$\Pi_{comb}$	$\Pi_{comb}$

**Table 1.** Independent variables held constant in previous investigations.

regards data volume and time involved was creating and running a program that steps through the various parameter values and determining optimum points. Only the optimum points were stored, resulting in one set that contained all the necessary data for constructing the optimum performance maps presented in this work.

For each parameter, a realistic range of variation was investigated. The operating range for the combustor outlet temperature was from about 700 K to 3000 K, which is the approximate limit for turbine materials. Table 2 lists the range for each independent variable. This investigation maintained  $\eta_{WE}$  and  $\eta_{WP}$  constant at 0.83.

Range for Independent Variables			
Cases A, B, and D	Range	Cases C and E	Range
R	1-26.5	R	1-26.5
$T_4$	700-2500 K	$T_3$	700-3000 K
$\eta_{PC}$	0.6-0.95	$\eta_{PC}$	0.55-0.95
$\eta_{PT}$	0.55-0.95	$\eta_{PT}$	0.55-0.95
$\Pi_{comb}$	0.55-0.95	$\Pi_{comb}$	0.55-0.95

**Table 2.** Range used in this investigation for independent variables.

## Results and Discussion

There are three objectives that this investigation focused on. The first objective is achieving the maximum *absolute performance* of the engine. The second objective is achieving the maximum *absolute improvement* of the wave rotor-topped engine over the baseline engine. The third objective is achieving the maximum *relative improvement* of the topped engine compared to the baseline engine. In addition, the term “optimizing” in this text refers to locating the maximum  $w$  and  $\eta_{th}$  and the minimum SFC and R.

### Cases A, B, and D

#### (1) Turbine Inlet Temperature

Shown in Fig. 3a are the results of varying  $T_4$ . Using the approach stated above,  $T_4$  and PRW were fixed while R was varied to locate one optimum point. Then  $T_4$  and PRW were changed incrementally and fixed and the process repeated to find all the other points displayed. The values of the constant parameters were  $\eta_{PC}=\eta_{PT}=0.9$  and  $\Pi_{comb}=0.95$ . Optimum thermal efficiency lines of constant  $T_4$  are shown as bold light green lines, and thermal efficiency lines of constant OPR are shown as thin dark green broken lines. Specific work lines of constant  $T_4$  are shown as bold blue lines, and specific work lines of constant OPR are shown as thin purple broken lines. Similarly, specific fuel

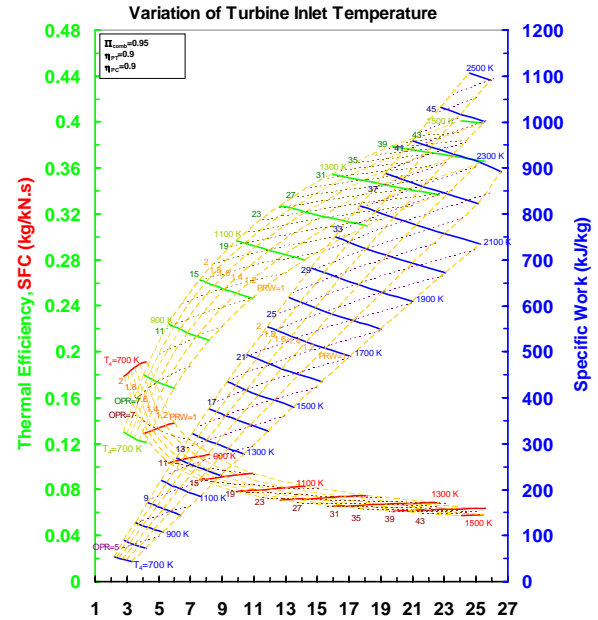


**Figure 3a.** Optimum points for variation of  $T_4$  for cases A, B, and D. Compressor pressure ratio is the variable on the independent axis.

consumption lines of constant  $T_4$  are shown as bold red lines, and specific fuel consumption lines of constant OPR are shown as thin brown broken lines. Lines of constant OPR could be shown on all following figures, but for better readability they are omitted in all other figures for cases A, B, and D. All lines of constant PRW are shown as thin broken yellow lines. For topped ( $PRW>1$ ) and untopped ( $PRW=1$ ) engines, as  $T_4$  increases, also  $\eta_{th}$ ,  $w$ , OPR, and R increases, while SFC decreases. Respectively, Fig. 3b and 3c show the absolute and relative changes in  $\eta_{th}$ ,  $w$ , and SFC compared to the baseline engine. As  $T_4$  increases, the absolute gain in  $\eta_{th}$  and  $w$  increases, while the gain (absolute decrease) in SFC decreases. For the relative values this trend is the same for SFC but reverses for  $\eta_{th}$  and  $w$ .

The absolute gain (decrease) in compressor pressure ratio for each objective function also increases with increasing  $T_4$ , while the trends for relative gain are reversed. Absolute and relative increases in compressor pressure ratio for each objective function are shown in Figure 3d and 3e, respectively.

#### (2) Polytropic Compressor Efficiency

Figure 4 displays the optimum points for varying polytropic compressor efficiency. Similar to Fig. 3, the procedure was used where  $\eta_{PC}$  and PRW were fixed while R varied. The optimum result was one point in Fig. 4. Then  $\eta_{PC}$  and PRW were incrementally fixed and R was varied again. As

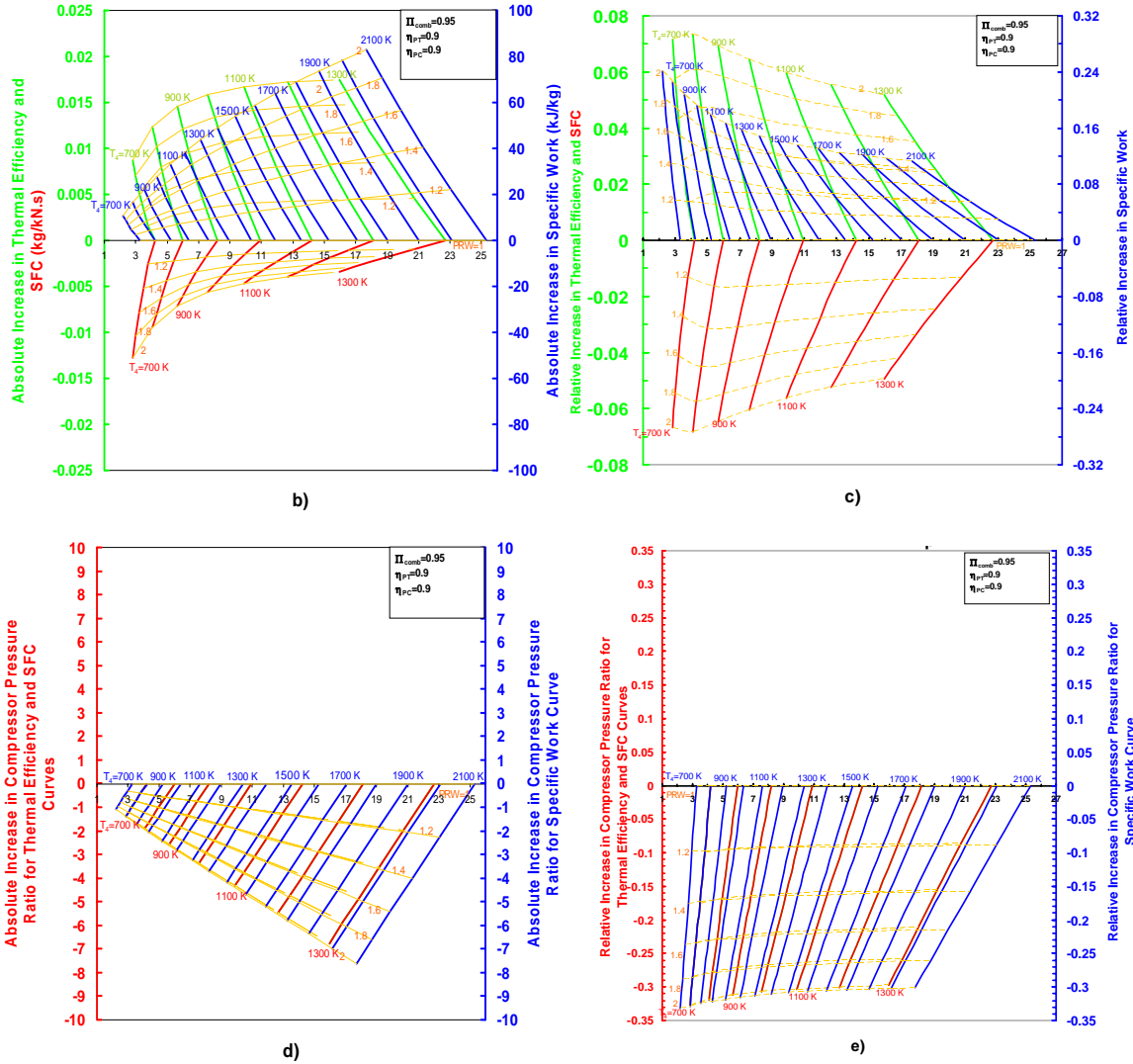


**Figure 3.** Optimum points for variation of  $T_4$  for cases A, B, and D. Compressor pressure ratio is the variable on the independent axis. Figure 3b and 3c are the absolute and relative gain of the objective functions, respectively. Figure 3d and 3e are absolute and relative change in compressor pressure ratio for the objective functions, respectively.

polytropic compressor efficiency increases, so does  $\eta_{th}$ ,  $w$ , and  $R$ , while SFC decreases. The constant parameter values were  $T_4=1000$  K,  $\eta_{PT}=0.9$ , and  $\Pi_{comb}=0.95$ . Other figures derived from the data in Figure 4 displaying absolute and relative gain could also be shown for the variation of  $\eta_{PC}$ . Such figures were used in the data analysis.

### (3) Polytropic Turbine Efficiency

Figure 5 displays the optimum points for varying polytropic turbine efficiency. As polytropic turbine efficiency increases, so does  $\eta_{th}$ ,  $w$ , and  $R$ , while SFC decreases. The constant parameter values were  $T_4=1000$  K,  $\eta_{PC}=0.9$ , and  $\Pi_{comb}=0.95$ . Similar to Fig. 4 and 6, other figures that are derived from the

data in Fig. 5 are used in the analysis but are not shown here.

### (4) Combustor Loss

Figure 6 displays the optimum points for varying combustor loss. By increasing  $\Pi_{comb}$ ,  $\eta_{th}$  and  $w$  also increase while SFC decreases. Interestingly,  $R$  for optimum  $w$  decreases with increasing  $\Pi_{comb}$  while  $R$  values for  $\eta_{th}$  and SFC increase. The constant parameter values were  $T_4=1000$  K and  $\eta_{PC}=\eta_{PT}=0.9$ .

#### (a) Thermal Efficiency

- The optimum design space for absolute performance of  $\eta_{th}$  is at high  $T_4$ , high  $\eta_{PT}$ , high  $\eta_{PC}$ , and high  $\Pi_{comb}$ . The optimum space for absolute

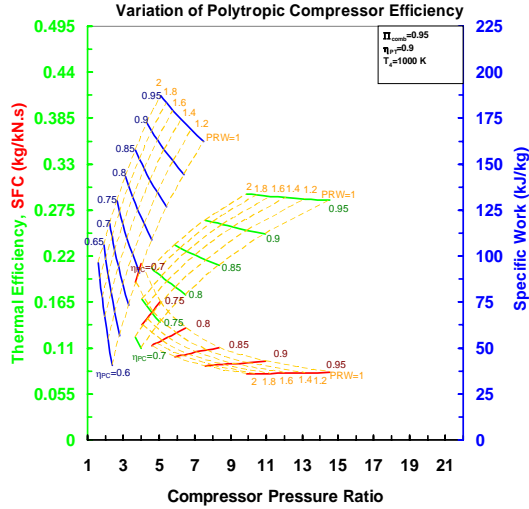


**Figure 4.** Optimum points for variation of polytropic compressor efficiency for cases A, B, and D.

performance of R is at low  $T_4$ , low  $\eta_{PT}$ , low  $\eta_{PC}$ , and low  $\Pi_{comb}$ .

- The optimum space for absolute increase in  $\eta_{th}$  of the topped engine over the baseline engine is at high  $T_4$ , low  $\eta_{PT}$ , low  $\eta_{PC}$ , and low  $\Pi_{comb}$ . For absolute decrease in R of the topped engine over the baseline engine, the space is at high  $T_4$ , high  $\eta_{PT}$ , high  $\eta_{PC}$ , and high  $\Pi_{comb}$ .
- The optimum space for relative increase in  $\eta_{th}$  is at an intermediate  $T_4$ , low  $\eta_{PT}$ , low  $\eta_{PC}$ , and low  $\Pi_{comb}$ . For relative decrease in R of the topped engine over the baseline engine, the space is low  $T_4$ , high  $\eta_{PT}$ , high  $\eta_{PC}$ , and high  $\Pi_{comb}$ .

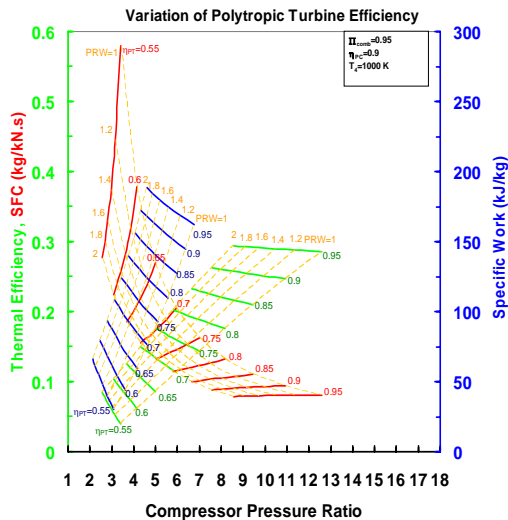


**Figure 5.** Optimum points for variation of polytropic turbine efficiency for cases A, B, and D.

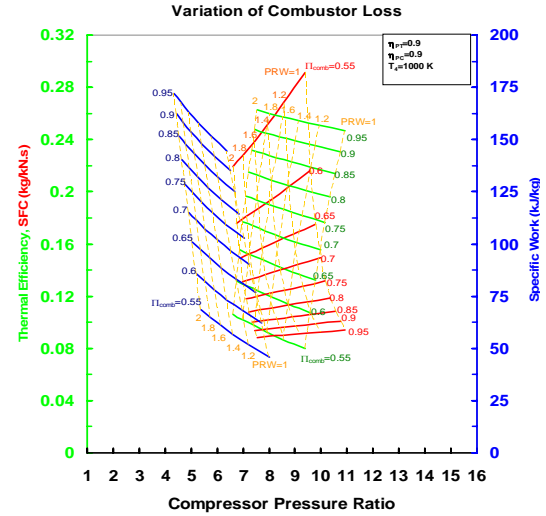


**Figure 6.** Optimum points for variation of combustor loss for cases A, B, and D

### (b) Specific Work

- For absolute performance of w, the optimum space is the same as the space for  $\eta_{th}$ . For the absolute performance of R, the design space is the same except that it occurs at high  $\Pi_{comb}$ .
- The optimum space for absolute increase in w of the topped engine over the baseline engine is the same as for  $\eta_{th}$  except that it occurs at high  $\eta_{PT}$ . The design space for absolute decrease in R of the topped engine over the baseline engine is also the same as for  $\eta_{th}$  except it occurs at low  $\eta_{PT}$ .
- The optimum design space for relative increase in w is the same as for  $\eta_{th}$  except at low  $T_4$ . The space for R is the same as for  $\eta_{th}$  except at an intermediate  $\eta_{PT}$ , intermediate  $\eta_{PC}$ , and low  $\Pi_{comb}$ .

### (c) Specific Fuel Consumption

- The optimum space for absolute performance for SFC and for R is the same as that for  $\eta_{th}$ .
- The optimum space for absolute decrease in SFC of the topped engine over the baseline engine is the same as that for  $\eta_{th}$  except it occurs at low  $T_4$ . The space for absolute decrease in R of the topped engine over the baseline engine is the same as that for  $\eta_{th}$ .
- The optimum space for relative decrease in SFC and R is the same as that for  $\eta_{th}$ .

## Cases C and E

### (1) Turbine Inlet Temperature

Figures 7-10 display the optimum space for cases C and E. The trends are similar to those for cases A, B, and D, but are not exactly the same. In

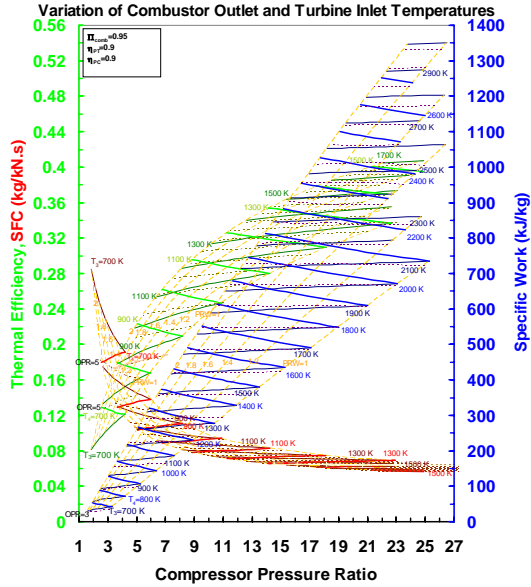


**Figure 7.** Variation of turbine inlet temperature for cases C and E.

Fig. 7, optimum thermal efficiency lines of constant  $T_4$  are shown as bold light green lines, lines of constant  $T_3$  are shown in thin medium green, and thermal efficiency lines of constant OPR are shown as thin dark green broken lines. Lines of constant  $T_3$  are displayed for cases C and E because for these cases,  $T_3$  is maintained the same as the baseline  $T_{4b}$ . That is why the lines of equal  $T_4$  and  $T_3$  merge at  $PRW=1$  (the baseline engine). Lines of constant  $T_4$  were used so that comparisons could be made to cases A, B, and D. Specific work lines of constant  $T_4$  are shown as bold blue lines, specific work lines of constant  $T_3$  are shown in thin dark blue, and specific work lines of constant OPR are shown as thin purple

**Variation of Polytropic Turbine Efficiency**

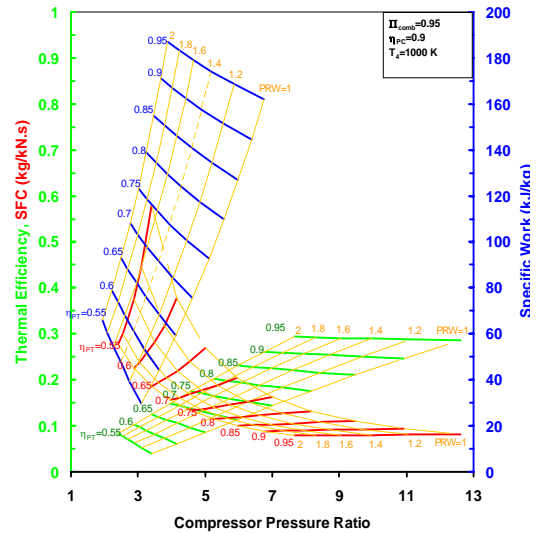


**Figure 9.** Variation of polytropic turbine efficiency for cases C and E.

broken lines. Similarly, specific fuel consumption lines of constant  $T_4$  are shown as bold red lines, specific fuel consumption lines of constant  $T_3$  are shown in thin dark red, and specific fuel consumption lines of constant OPR are shown as thin brown broken lines. Lines of constant OPR and constant  $T_3$  could be shown on all following figures, but for the sake of clarity they are only displayed for cases C and E in Fig. 7. All lines of constant PRW are shown as broken thin yellow lines. All of the figures associated with absolute and relative gain of  $\eta_{th}$ ,  $w$ , SFC, and  $R$  are used in the analysis of the data but are not shown here.

**Variation of Polytropic Compressor Efficiency**

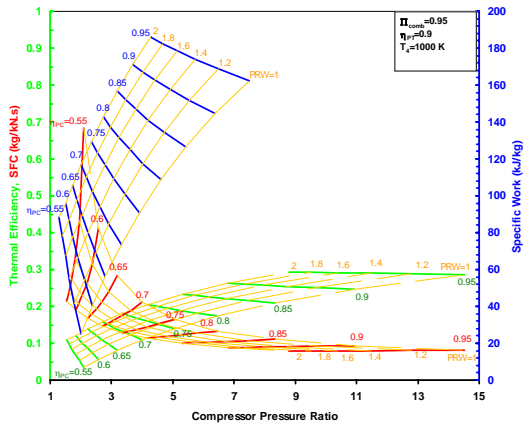


**Figure 8.** Variation of polytropic compressor efficiency for cases C and E.

**Variation of Combustor Loss**

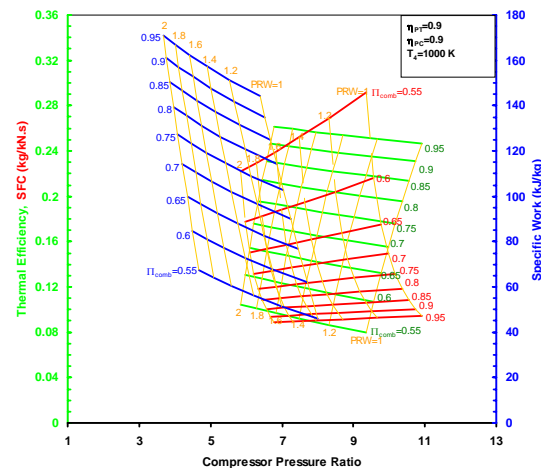


**Figure 10.** Variation of combustor loss for cases C and E.

As is shown in Fig. 7, increasing turbine inlet temperature also increases  $\eta_{th}$ ,  $w$ , OPR, and R, but decreases SFC. The same is true for increasing  $T_3$ . However, maintaining a constant  $T_3$  while increasing PRW causes a decrease in  $\eta_{th}$  and  $w$ , and an increase in SFC. The opposite is true for maintaining a constant  $T_4$  while increasing PRW.

### (2) Polytropic Compressor Efficiency

Figure 8 shows the effect increasing polytropic compressor efficiency has on  $\eta_{th}$ ,  $w$ , SFC, and R. As  $\eta_{PC}$  increases, so does  $\eta_{th}$ ,  $w$ , and R, but SFC decreases. The constant parameter values were  $\eta_{PC}=\eta_{PT}=0.9$  and  $\Pi_{comb}=0.95$ .

### (3) Polytropic Turbine Efficiency

The results of varying polytropic turbine efficiency are shown in Fig. 9. Increasing  $\eta_{PT}$  also causes an increase in  $\eta_{th}$ ,  $w$ , and R, but a decrease in SFC. The constant parameter values were  $T_4=1000$  K,  $\eta_{PC}=0.9$  and  $\Pi_{comb}=0.95$ .

### (4) Combustor Loss

Increasing combustor loss causes an increase in  $\eta_{th}$  and  $w$ , but a decrease in SFC. Similar to Cases A, B, and D, there is actually a decrease in the R value for specific work with increasing  $\Pi_{comb}$ . However, the R values for SFC and  $\eta_{th}$  increase with increasing  $\Pi_{comb}$ . This can be observed in Fig. 10. The values of the parameters maintained constant are  $\eta_{PC}=\eta_{PT}=0.9$  and  $\Pi_{comb}=0.95$ .

#### (a) Thermal Efficiency

- The optimum space for  $\eta_{th}$  is the same as for cases A, B, and D.

#### (b) Specific Work

- The optimum space for  $w$  is the same as for cases A, B, and D, but for relative increase it occurs at high  $T_4$ , high  $\eta_{PT}$ , high  $\eta_{PC}$ , and high  $\Pi_{comb}$ .

#### (c) Specific Fuel Consumption

- The optimum space for SFC is the same as for cases A, B, and D

### All Cases

The comparisons between the two main sets of data, each objective function, and the independent variables are shown in Table 3. The comparisons in the table are derived from the trends in Figures 3-10. The results from all cases in general show the same performance trends, however there are differences between cases A, B and D, and cases C and E for specific work trends. The performance trends for specific work, thermal efficiency, and specific fuel

consumption also are the same except for several instances.

## Conclusions

A series of optimum points was obtained for three objective functions of wave rotor-topped gas turbine performance: thermal efficiency, specific work, and specific fuel consumption that were expressed in absolute value, absolute improvement, and relative improvement. The independent variables were  $T_3$ ,  $T_4$ , OPR, PRW,  $\eta_{PC}$ ,  $\eta_{PT}$ , and  $\Pi_{comb}$ . A total of 5 cases were investigated; three which maintain the same turbine inlet temperature as the baseline engine (A, B and D) and two which maintain the same combustor outlet temperature as the baseline engine (C and E). The conclusions are:

1. There are two main sets of optimum points: one for cases A, B, and D, and one for cases C and E.
2. The optimum trends for thermal efficiency and specific fuel consumption are the same for all cases.
3. The optimum trends for specific work are nearly the same for all cases, but some exceptions exist.
4. Besides several exceptions, the optimum performance trends are the same for thermal efficiency, specific work, and specific fuel consumption
5. In general, high values for  $T_4$ ,  $\eta_{PC}$ ,  $\eta_{PT}$ , and  $\Pi_{comb}$  result in high gains for the objective functions, while low values of those parameters result in small compressor pressure ratios.
6. In the investigated design space and with constant  $\eta_{WE}$  and  $\eta_{WP}$ , increasing PRW always increases the maximum performance of the gas turbine engine.

Wave rotor topping of gas turbine engines is beneficial throughout a wide range of gas turbine sizes, efficiencies, and operating conditions. Because the focus of the investigation is on wave rotor *enhancement* of gas turbine engines, the most significant conclusions can be drawn from the relative performance improvement of objective functions. From this perspective, small gas turbines with low component efficiencies, low temperatures occupy the optimum design space for wave rotor-topping.

		Objective					
		Absolute Performance		Wave Rotor-Topped Engine Compared to Baseline			
		high $\eta_{th}$	low R	absolute increase in $\eta_{th}$	absolute decrease in R	relative increase in $\eta_{th}$	relative decrease in R
Thermal Efficiency	high $T_4$	All Cases		All Cases	All Cases		
	mid $T_4$					All Cases	
	low $T_4$		All Cases				All Cases
	high $\eta_{PC}$	All Cases			All Cases		All Cases
	mid $\eta_{PC}$						
	low $\eta_{PC}$		All Cases	All Cases		All Cases	
	high $\eta_{PT}$	All Cases			All Cases		All Cases
	mid $\eta_{PT}$						
	low $\eta_{PT}$		All Cases	All Cases		All Cases	
	high $\Pi_{comb}$	All Cases			All Cases		All Cases
mid $\Pi_{comb}$							
low $\Pi_{comb}$		All Cases	All Cases		All Cases		
		high w	low R	absolute increase in w	absolute decrease in R	relative increase in w	relative decrease in R
Specific Work	high $T_4$	All Cases		All Cases	All Cases		Cases C and E
	mid $T_4$						
	low $T_4$		All Cases			All Cases	Cases A, B, and D
	high $\eta_{PC}$	All Cases			All Cases		Cases C and E
	mid $\eta_{PC}$						Cases A, B, and D
	low $\eta_{PC}$		All Cases	All Cases		All Cases	
	high $\eta_{PT}$	All Cases			All Cases		Cases C and D
	mid $\eta_{PT}$						Cases A, B, and D
	low $\eta_{PT}$		All Cases	All Cases		All Cases	
	high $\Pi_{comb}$	All Cases	All Cases	All Cases			Cases C and E
mid $\Pi_{comb}$							
low $\Pi_{comb}$				All Cases	All Cases	Cases A, B, and D	
		low SFC	low R	absolute decrease in SFC	absolute decrease in R	relative decrease in SFC	relative decrease in R
Specific Fuel Consumption	high $T_4$	All Cases			All Cases		
	mid $T_4$					All Cases	
	low $T_4$		All Cases	All Cases			All Cases
	high $\eta_{PC}$	All Cases			All Cases		All Cases
	mid $\eta_{PC}$						
	low $\eta_{PC}$		All Cases	All Cases		All Cases	
	high $\eta_{PT}$	All Cases			All Cases		All Cases
	mid $\eta_{PT}$						
	low $\eta_{PT}$		All Cases	All Cases		All Cases	
	high $\Pi_{comb}$	All Cases			All Cases		All Cases
mid $\Pi_{comb}$							
low $\Pi_{comb}$		All Cases	All Cases		All Cases		

**Table 3.** Comparison between the independent variables and the objective functions for each case.

### References

[1] Wilson, J., Paxson, D. E., 1993, "Jet Engine Performance Enhancement Through Use of a Wave-Rotor Topping Cycle," NASA TM-4486.

[2] Akbari, P., Müller, N., 2004, "A Review of Wave Rotor Technology and Recent Developments," 2003 ASME International Mechanical Engineering Conference, ASME IMECE2004-60082.

[3] Akbari, P., Müller, N., 2003, "Performance Investigation of Small Gas Turbine Engines Topped with Wave Rotors," 2003 AIAA/ASME/SAE/ASEE Joint Propulsion Conference and Exhibit, AIAA Paper 2003-4414.

[4] Akbari, P., Müller, N., 2003, "Performance Improvement of Small Gas Turbines Through Use of Wave Rotor Topping Cycles," 2003 International ASME/IGTI Turbo Exposition, ASME Paper GT2003-38772.

[5] Guzzella, L., Martin, R., 1998, "The Save Engine Concept," MTZ Report 10, pp. 9-12.

[6] Akbari, P., 2004, "Performance Prediction and Preliminary Design of Wave Rotors Enhancing Gas Turbine Cycles," Ph.D. Thesis, Michigan State University, MI.